

Analyst

Accepted Manuscript



This is an *Accepted Manuscript*, which has been through the Royal Society of Chemistry peer review process and has been accepted for publication.

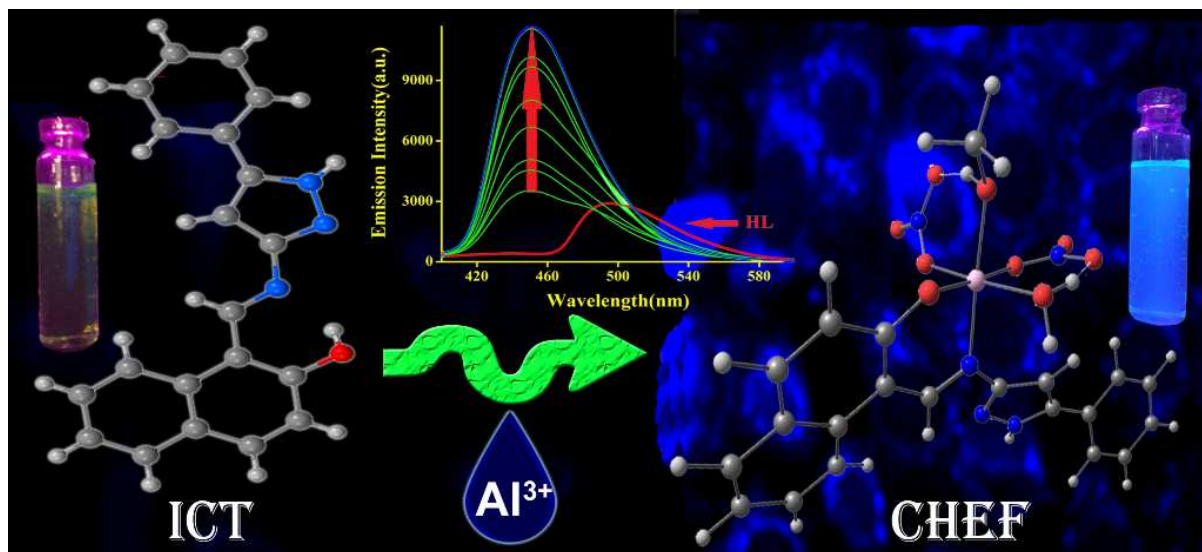
Accepted Manuscripts are published online shortly after acceptance, before technical editing, formatting and proof reading. Using this free service, authors can make their results available to the community, in citable form, before we publish the edited article. We will replace this *Accepted Manuscript* with the edited and formatted *Advance Article* as soon as it is available.

You can find more information about *Accepted Manuscripts* in the [Information for Authors](#).

Please note that technical editing may introduce minor changes to the text and/or graphics, which may alter content. The journal's standard [Terms & Conditions](#) and the [Ethical guidelines](#) still apply. In no event shall the Royal Society of Chemistry be held responsible for any errors or omissions in this *Accepted Manuscript* or any consequences arising from the use of any information it contains.

Graphical abstract

A new naphthalene-pyrazol conjugate (HL) has been designed and crystallographically characterized and it behaves as an Al(III) ions selective chemosensor in 100 mM HEPES buffer (water/DMSO:5/1, v/v) at biological pH in short response time; and it is an efficient biomarker in detecting Al(III) ions in living cells with no cytotoxic effect.



Cite this: DOI: 10.1039/c0xx00000x

www.rsc.org/xxxxxx

ARTICLE TYPE

A naphthelene-pyrazol conjugate: Al(III) ion selective blue shifting chemosensor applicable as biomarker in aqueous solution

Manjira Mukherjee,^a Siddhartha Pal,^a Somenath Lohar,^a Buddhadeb Sen,^a Supriti Sen,^a Samya Banerjee,^b Snehasis Banerjee^c and Pabitra Chattopadhyay^{a*}

5 Received (in XXX, XXX) Xth XXXXXXXXXX 20XX, Accepted Xth XXXXXXXXXX 20XX

DOI: 10.1039/b000000x

A newly synthesized and crystallographically characterized naphthelene-pyrazol conjugate, *1-[(5-phenyl-1H-pyrazole-3-ylimino)-methyl]-naphthalen-2-ol* (**HL**) behaves as an Al(III) ions selective chemosensor through ICT-CHEF processes in 100 mM HEPES buffer (water /DMSO : 5/1, v/v) at biological pH with almost no interference of other competitive ions. This mechanism is nicely studied from electronic, fluorimetric and ¹HNMR titration. This probe (**HL**) behaved as a highly selective fluorescent sensor for Al(III) ions as low as 31.78 nM within a very short responsive time (15-20 s). The sensor (**HL**) having no cytotoxicity is also efficient to detect the distribution of Al(III) ions in Hela cells by developing image under fluorescence microscope.

15 Introduction

Aluminium is the third most prevalent (8.3% by weight) metallic element in the earth. Aluminium compounds are extensively used in the paper industry,¹ in dye production,² in the textile industry,³ as a component of many cosmetic preparations and aluminium salts are currently utilized in alimentary industry.^{4,5} Aluminium compounds are also frequently utilized as pharmaceutical drugs in human and veterinary medicine.⁶ Aluminium can be toxic to humans in excessive amounts. Excess aluminium is acquired by the use of antiperspirants and deodorants,^{4,7} aluminium cookware, cans, bleached flour, antacids and drinking water supplies.⁸ After absorption, aluminium is generally dispensed to all tissues in humans and animals, and accumulates in the bone. The iron binding proteins (e.g. transferrin C1 and C2, and ferritin etc.) are the main carriers of Al(III) ions in plasma^{9a,b} and Al(III) ions can enter the brain^{9c} and reach the placenta^{9d} and fetus.^{9e} Al(III) ions may persist for a very long time in various organs and tissues before it is excreted in the urine. Many symptoms of aluminium toxicity mimic those of Alzheimer's disease and osteoporosis. Colic, rickets, gastrointestinal problems, interference with the metabolism of calcium, extreme nervousness, anemia, headaches, decreased liver and kidney function, memory loss, speech problems, softening of the bones, aching muscles and even to risk the cancer of lung and bladder can all be caused by aluminium toxicity.¹⁰⁻¹⁵ Thus, aluminium should be regarded as a toxic metal and its concentration in environment ought to be monitored. World Health Organization (WHO) listed aluminium as one of the food pollution sources and limited aluminium concentration upto 7.41 mM in drinking water. The FAO/WHO Joint Expert

Committee on Food Additives recommended a maximum daily intake of aluminium of 3-10 mg per day/kg-body mass. Furthermore, it is believed that almost 40% of the world's acid soils are polluted by the effects of aluminium toxicity, which is the key factor for hampering plant (i.e., crop) performance on the acid soils.^{16,17}

Considering the above fact, it is evident that detection of Al ions is indispensable in controlling its concentration levels. Several conventional methods with moderate sensitivity for Al(III) ions detection based on atomic absorption spectroscopy (AAS), chromatographic and spectro-photometric techniques have been developed.¹⁸ The spectrofluorimetric method has received considerable attention in recent years due to its simplicity, high sensitivity and real-time monitoring with a low response time.¹⁹⁻²¹ There are several fluorescent sensors for Al(III) ions with several disadvantages including complicated synthetic procedures, poor water solubility, insensible to biological system having interferences often by other ions. More over, most of them are chelation-enhanced fluorescence (CHEF)/photoinduced electron transfer (PET)/FRET based sensor.²²

In this work, we focused on Al(III) ion sensing with the developed Schiff base, *1-[(5-phenyl-1H-pyrazol-3-ylimino)-methyl]-naphthalen-2-ol* (**HL**) derived by the condensation of *3-amino-5-phenylpyrazole* with *2-hydroxy naphthaldehyde* for sensor investigation, where **HL** is chosen due to its characteristics of high emission, excellent photostability, and significant fluorescent behaviour in the visible region. Herein, we describe this **HL** as a chemosensor selective for Al(III) ions, utilizing "turn-on" fluorescence shifting. Interestingly, the presence of an excess of the other metal ions, viz. alkali [Na(I), K(I)], alkaline earth [Mg(II), Ca(II)], and transition metal ions [Cr(III), Mn(II), Fe(III), Co(II), Ni(II), Cu(II), Zn(II), Cd(II),

Hg(II)] and Pb(II) ions do not affect this behaviour of **HL** observed in presence of Al(III) ions due to the selective formation of **HL-Al complex**.

Experimental

5 Materials and physical measurements

All of the solvents were of analytical grade. The elemental analyses (C, H and N) were performed on a Perkin Elmer 2400 CHN elemental analyzer. A Shimadzu (model UV-1800) spectrophotometer was used for recording electronic spectra. IR spectra were recorded using Prestige-21 SHIMADZU FTIR spectrometer. ¹H NMR spectrum of organic moiety was obtained on a JEOL 400 spectrometer using DMSO-d₆ solution. High Resolution (HR) mass spectra were recorded on a Qtof Micro YA263 mass spectrometer. A Systronics digital pH meter (model 335) was used to measure the pH of the solution and the adjustment of pH was done using either 50 mM HCl or KOH solution. Steady-state fluorescence emission and excitation spectra were recorded with a Hitachi-4500 spectrofluorimeter. The fluorescence spectra of the titration of aluminium ion with organic moiety were obtained at an emission wavelength of 450 nm in the fluorimeter. Time-resolved fluorescence lifetime measurements were performed using a HORIBA JOBIN Yvon picosecond pulsed diode laser-based time-correlated single-photon counting (TCSPC) spectrometer from IBH (UK) at λ_{exc} = 340 nm and MCP-PMT as a detector. Emission from the sample was collected at a right angle to the direction of the excitation beam maintaining magic angle polarization (54.71). The full width at half-maximum (FWHM) of the instrument response function was 250 ps, and the resolution was 28.6 ps per channel. Data were fitted to multiexponential functions after deconvolution of the instrument response function by an iterative reconvolution technique using IBH DAS 6.2 data analysis software in which reduced w₂ and weighted residuals serve as parameters for goodness of fit.

The luminescence property of the sensor was investigated in water: DMSO (5:1, v/v) solvent. pH study was done in 100 mM HEPES buffer solution by adjusting pH with HCl or NaOH. *In vivo* study was performed at biological pH ~7.4 with 100 mM HEPES buffer solution. The stock solutions (~ 10⁻² M) for the selectivity study of the probe (**HL**) towards different metal ions were prepared taking nitrate salts of sodium(I), potassium(I), copper(II), chromium(III), silver(I); acetate salt of manganese(II), zinc(II); chloride salts of nickel(II), cobalt(II), mercury(II), calcium(II), magnesium(II), iron(III) and iron(II) sulphate; in water : DMSO (5 : 1, v/v) solvent. In this selectivity study the amount of these metal ions was a hundred times greater than that of the probe used. Fluorescence titration was performed with aluminium nitrate in water: DMSO (5: 1, v/v) solvent varying the metal concentration 0 to 15 μM and the probe concentration was 10 μM.

Preparation of 1-[(5-phenyl-1H-pyrazol-3-ylimino)-methyl]-naphthalen-2-ol (**HL**)

To ethanolic solution of 3-amino-5-phenylpyrazole (0.79 g, 5.0 mmol) (25 mL) 2-hydroxy naphthaldehyde (0.86 g, 5.0 mmol) in 25 mL of ethanol was added dropwise at room temperature under nitrogen atmosphere. The resulting mixture was refluxed for 6.0 h. The yellow coloured precipitate of the compound (**HL**) was collected through filtration after reducing the solvent on slow evaporation. Single crystals of the compound were obtained from the ethanolic solution. C₂₀H₁₅N₃O: M.P.: 245°C. Anal. Found: C, 76.14; H, 4.69; N, 13.76; Calc.: C, 76.66; H, 4.82; N, 13.41. HR-MS: [M + H]⁺, m/z, 314.1286 (100%) (calcd.: m/z, 314.12. IR (KBr, cm⁻¹): ν_{OH}, 3446.79, ν_{NH}, 3097.68, ν_{CH=N}, 1624.06. ¹H NMR (400Hz DMSO-d₆): δ, 15.62 (s, 1H); 13.42 (s, 1H); 9.830 (s, 1H); 8.50 (d, 1H, J = 8.4); 7.978 (d, 1H, J = 7.732); 7.87-7.81 (m, 3H); 7.60 (t, 1H, J=7.6); 7.52 (t, 2H, J=6.88); 7.40 (t, 2H, J=6.88); 7.34 (s, 1H); 7.12 (d, 1H, J = 8.4). Yield: 90%.

70 Preparation of the aluminium (III) complex (**HL-Al**)

To a methanolic solution of **HL** (313.0 mg, 1.0 mmol) solid aluminium(III) nitrate nonahydrate (375 mg, 1.0 mmol) was added at a time and then the reaction mixture was stirred at ambient temperature for 6.0 h. The resulting solution thus obtained was then kept aside for slow evaporation at room temperature. After a few days, a greenish yellow coloured complex was obtained by washing thoroughly with cold methanol and water, and then dried *in vacuo*.

C₂₂H₂₄AlN₅O₉: Anal. Found: C, 49.69; H, 4.39; N, 13.67; Calc.: C, 49.91; H, 4.57; N, 13.23; IR (cm⁻¹): ν_{OH}, 3471.67(b); ν_{NO₃}, 1382.96. Conductivity (Λ_m, M⁻¹ cm⁻¹) in MeOH: 57. ESI-MS in methanol: [M + H]⁺, m/z, 514.2007 (obsd. with 8% abundance) (calcd.: m/z, 514.44) and [M + Na]⁺, m/z, 536.24 (obsd. with 12% abundance) where M = [Al(L)(NO₃)₂(H₂O)(CH₃OH)]. ¹H NMR (400Hz DMSO-d₆): δ, 15.59 (s, 1H); 13.39 (s, 1H); 9.82 (s, 1H); 8.48 (d, 1H, J = 8.4); 7.97-7.93 (m, 2H); 7.87-7.81 (m, 3H); 7.58 (t, 1H, J = 7.6); 7.48 (t, 2H, J = 6.88); 7.40 (t, 2H, J = 6.88); 7.29 (s, 1H); 7.12 (d, 1H, J = 8.4); 4.22 (s, 1H); 3.16 (s, 3H) Yield: 75%.

90 X-ray data collection and structural determination[‡]

The single crystals were obtained from the solution of the compound (**HL**) in methanol on slow evaporation. X-ray data were collected on a Bruker's Apex-II CCD diffractometer using Mo Kα (λ=0.71069). The data were corrected for Lorentz and polarization effects and empirical absorption corrections were applied using SADABS from Bruker. A total of 8503 reflections were measured out of which 3602 were independent and 1282 were observed [I > 2 σ(I)]. The structure was solved by direct methods using SIR-92²³ and refined by full-matrix least squares refinement methods based on F², using SHELX-97.²⁴ All non-hydrogen atoms were refined anisotropically. All calculations were performed using Wingx²⁵ package. Important crystal and refinement parameters are given in **Table 1**.

Preparation of cell and *in vitro* cellular imaging with **HL**

Human cervical cancer cell, HeLa cell was used throughout the study. HeLa cells were maintained in Dulbecco's Modified Eagle's Medium (DMEM), supplemented with 10% fetal

bovine serum (FBS), 100 $\mu\text{g}\cdot\text{ml}^{-1}$ of penicillin, 100 $\mu\text{g}\cdot\text{ml}^{-1}$ of streptomycin and 2 mM Glutamax at 37 °C in a humidified incubator at 5% CO₂. The adherent cultures were grown as monolayer and passaged once in 4-5 days by trypsinizing with 0.25% Trypsin-EDTA. HeLa cells (4 x 10⁴ cells/mm²), plated on cover slips, were incubated with **HL** (10, 5 and 2 μM , 1% DMSO) for 30 min. After washing with 50 mM phosphate buffer, pH 7.4 containing 150 mM NaCl (PBS), required volumes of aluminium nitrate stock solution in DMSO were added such that final [Al(NO₃)₃] adjusted to 2.0 μM , 5.0 μM and 10.0 μM (DMSO will be 1%) and incubated for 30 min. The cells were fixed with 4% paraformaldehyde for 10 min at room temperature (RT). After washing with PBS, mounted in 90% glycerol solution containing Mowiol, an anti-fade reagent, and sealed. Images were acquired using Apotome.2 fluorescence microscope (Carl Zeiss, Germany) using an oil immersion lens at 63 X magnification. The images were analyzed using the AxioVision Rel 4.8.2 (Carl Zeiss, Germany) software.²⁶

20 Cell Cytotoxicity Assay

Cytotoxicity measurements of the ligand was carried out using MTT assay which is based on the cleavage of the tetrazolium ring of MTT by mitochondrial dehydrogenases in the viable cells to form formazan as dark blue membrane impermeable species that can be quantified at 540 nm in DMSO solution giving a measure of the number of viable cells.²⁷ Human cervical cancer cell (HeLa) plated in 96-well culture plates were treated with different concentrations of the ligand and incubated for 6 h followed by addition of 25 μl of 4 mg ml⁻¹ of MTT to each well and incubated for an additional 3 h. The culture medium was discarded and a 200 μl volume of DMSO was added to dissolve the formazan crystals. The absorbance at 540 nm was determined using an ELISA microplate reader (BioRad, Hercules, CA, USA). The cytotoxicity of the complexes was measured as the percentage ratio of the absorbance of the treated cells over the untreated controls. The IC₅₀ value was determined by nonlinear regression analysis (GraphPad Prism).

Theoretical Calculation

The gradient-corrected DFT level involving the hybrid 3-parameter fit of exchange and correlation functionals of Becke (B3LYP) which includes the correlation functional of Lee, Yang, and Parr (LYP) was used. The standard split valence basis sets 6-31G(d) were applied for other atoms. Natural population analysis (NPA) (implemented in Gaussian 09 program) at B3LYP/6-31G(d) level was carried out to compute the charge on each atom.

Results and discussion

Synthesis and characterization

The organic moiety (**HL**) was synthesized by condensing an ethanolic solution of 3-amino-5-phenylpyrazole with 2-hydroxy naphthaldehyde in equimolar ratio (**Scheme 1**). The formulation of **HL** as shown in **Scheme 1** was established by physico-chemico and spectroscopic tools along with the detailed structural analysis by single crystal X-ray

crystallography. The probe is soluble in common polar organic solvents and sparingly soluble in water. The peaks obtained in ¹H NMR spectrum of **HL** have been assigned and these are in accordance with structural formula of the **HL** in the solution state (**Fig. S1**). The HR mass spectrum of the compound in methanol shows a peak at m/z 314.1286 with 100% abundance assignable to [M + H]⁺ (calculated value at m/z, 314.12) where M = molecular weight of **HL** (**Fig. S2**). IR spectrum of **HL** shows the characteristic stretching of O-H, N-H and C=N bonds (**Fig. S3**). An ORTEP view of the probe **HL** with the atom numbering scheme is illustrated in **Fig. 1**. The crystallographic data and the bond parameters (selected bond distances and angles) are listed in **Tables 1** and **2**, respectively. The bond lengths reported in **Table 2** indicate that C12-N2 bond distance (1.335 Å) is shorter than to that of C14-N3 (1.365 Å) but both values are larger than that of C11-N1 (1.294 Å) and shorter than C12-N1 (1.402 Å). The bond N3-H (0.86 Å) and O1-H (0.82 Å) distances are almost comparable.

To establish the fact of the formation of the aluminium(III) complex, (**HL-Al**) was isolated in solid state from the reaction of aluminium(III) nitrate and **HL** in 1:1 mole ratio in the methanol medium in stirring condition. The complex is soluble in methanol, DMSO and acetonitrile etc. The peaks obtained in ¹H NMR spectrum of aluminium(III) complex have been assigned and it is in accordance with structural formula of the aluminium complex **HL-Al** as [Al(L)(NO₃)₂(H₂O)(CH₃OH)] (**Fig. S4**). IR spectrum of **HL-Al** complex shows the characteristic stretching frequency of NO₃ group (**Fig. S5**). The considerably low value of the conductance (Λ_{∞} , 57 M⁻¹ cm⁻¹) of the complex in methanol at 300 K suggests that **HL-Al** exists as nonelectrolyte in solution state. The HR mass spectrum of the complex in methanol shows a peak at m/z, 514.2007 with 8% abundance, assignable to [M + H]⁺ (calculated value at m/z, 514.44) and [M + Na]⁺, m/z, 536.24 (obsd. with 12% abundance) where M = [Al(L)(NO₃)₂(H₂O)(CH₃OH)] (**Fig. S6**). Here, the organic moiety (**HL**) behaves as bidentate monobasic ligand. All these data confirm the composition of the complex **HL-Al** as [Al(L)(NO₃)₂(H₂O)(CH₃OH)].

To clarify the configurations of **HL** and **HL-Al** DFT calculations were performed (**Fig. S7**). The narrowing of the energy gap between the HOMO and LUMO of **HL-Al** compared to **HL** demonstrated the facile conversion as well as the extra stability of the **HL-Al** (**Fig. S8**). The contours of the electronic distribution in highest occupied molecular orbital (HOMO) and lowest unoccupied molecular orbital (LUMO) states of these molecules suggested a very little differences between compounds **HL** and **HL-Al** (**Figure S8**). Precisely, both HOMO and LUMO states of the **HL-Al** with comparing to **HL** revealed that the electrons are more delocalized towards the pyrazole groups than the naphthaldehyde unit in agreement with the hindrance of PET process, which results in the enhancement of fluorescence through CHEF (**Scheme 2**).²⁸

Spectral characteristics

Absorption study

The electronic spectrum of **HL** (10 μM) recorded in DMSO-

water HEPES buffer (1/5) (v/v) exhibited intense absorption-bands at higher energy below 400 nm corresponding to $\pi \rightarrow \pi^*$ (320 nm, $\epsilon = 9.76 \times 10^3$) and $n \rightarrow \pi^*$ (366 nm, $\epsilon = 7.52 \times 10^3$) transitions along with an intramolecular charge transfer band at 417 nm ($\epsilon = 3.36 \times 10^3$). On gradual addition of Al(III) ions, at first the peak at 417 nm gradually decreases up to the addition of 5.0 μM of Al(III) ions. Further addition of Al(III) ions, two new peaks appeared at *ca.* 380 nm and at *ca.* 405 nm were increased along with the red shift of 320 nm ($\pi \rightarrow \pi^*$ of free **HL**) towards 335 nm (**Fig. 2**). The new peak at 380 nm is generated probably due to the decrease of absorbance at 366 nm ($n \rightarrow \pi^*$ of free **HL**) and the peak at 405 nm attributable to the charge transfer band due to the blue shift of the charge transfer band at 417 nm of **HL**. This observation (**Fig. 2**) is in support of the formation of the **HL-Al** in the final solution state as the UV-vis spectrum of the isolated **HL-Al** formulated as $[\text{Al}(\text{L})(\text{NO}_3)_2(\text{H}_2\text{O})(\text{CH}_3\text{OH})]$ recorded in DMSO-water HEPES buffer (1/5) (v/v) exhibited absorption-bands at 335 nm ($\pi \rightarrow \pi^*$, $\epsilon = 1.094 \times 10^4$), 380 nm ($n \rightarrow \pi^*$, $\epsilon = 7.40 \times 10^3$) and 405 nm (charge transfer band, $\epsilon = 6.40 \times 10^3$). This blue shift phenomenon (Scheme 2) is due to the complex formation giving rise to a visual color change of the solution from yellow to colorless. (**Fig. S9**).

Emission study

The fluorescence emission spectra of **HL** at 450 nm ($\lambda_{\text{ex}} = 405$ nm) (**Fig. S10**) was very weak with a quantum yield of $\Phi = 0.1016$ but the emission intensity gradually increases with increase of added Al(III) ions. Addition of Al(III) ions (10 μM) to **HL** (10 μM), the intensity of the emission was increased with the enhancement of fluorescence quantum yield²⁹ by *ca.* 3.23 times ($\Phi = 0.329$) in ethanol medium, estimated by integrating the area under the fluorescence curves with the equation:

$$\phi_{\text{sample}} = \frac{\text{OD}_{\text{standard}} \times A_{\text{sample}}}{\text{OD}_{\text{sample}} \times A_{\text{standard}}} \times \phi_{\text{standard}}$$

The blue shift in emission spectra (*viz.* **Fig. 3**) after the gradual addition of Al(III) ions was due to reduced electron transfer (reduction of ICT, **Scheme 2**) from donor end (i.e. phenolic-OH end) of the **HL**.^{19,30} Further increment of addition of Al(III) ions, the new peak appeared at 450 nm is attributable for CHEF process.

There was almost no interference for the detection of Al(III) ions even in the presence of 100 equivalent concentration of alkali and alkaline earth metal ions (Na(I), K(I), Mg(II), Ca(II)), and 50 equivalent concentration of several transition metal ions (Mn(II), Fe(III), Co(II), Ni(II), Cu(II), Zn(II)) (**Fig. S11** and **S12**). Job's plot analysis (**Fig. 4**) revealed that *in situ* formed **HL** yield a 1:1 **HL-Al** complex. The binding constant (K , $5.18 \times 10^3 \text{ M}^{-1}$) was determined from the emission intensity data (**Fig. 5**) using the modified Benesi-Hildebrand equation corresponding to 1:1 stoichiometry.^{21,31}

$$1/(F_x - F_0) = 1/(F_{\text{max}} - F_0) + (1/K[C]) / (F_{\text{max}} - F_0)$$

where F_0 , F_x , and F_{∞} are the emission intensities of organic

moiety considered in the absence of Al(III) ions, at an intermediate Al(III) concentration, and at a concentration of complete interaction, respectively, and where $[C]$ is the concentration of Al(III) ions.

The fluorescence average lifetime measurement of organic moiety (**HL**) in presence and absence of Al(III) ion in the water-DMSO (5:1) medium indicates the gradual increase with increase of Al(III) ion concentration (**Fig. S13**). The average lifetimes were calculated to be 0.033 ns for only **HL**, 0.26 ns for the mixture of **HL**: Al(III) (1:0.5) and 0.61 ns **HL**: Al(III) (1:1). The strong binding of Al(III) with organic moiety reflected from the binding constant value, has played a key role for the selective chelation enhanced fluorescence (CHEF) in the presence of Al(III) ion. According to the equations: $\tau^{-1} = k_r + k_{\text{nr}}$ and $k_r = \Phi / \tau$,³² the radiative rate constant k_r and total non-radiative rate constant k_{nr} of the organic moiety, **HL** and aluminium(III) complex were listed in **Table S1**. The data suggest that the fluorescent enhancement is ascribed to the decrease of the ratio of k_{nr} / k_r from 8.84 for **HL** to 2.039 for **HL-Al** complex.

¹HNMR titration

In order to strengthen the above bonding pathway of Al(III) ions with **HL**, ¹HNMR titration was performed by addition of Al(III) ions to the DMSO-d₆ solution of **HL** and significant spectral changes were observed during addition of Al(III) ions (**Figs. S14** and **S15**). After the addition of 0.5 mM of Al(III) ions to the solution of 1.0 mM **HL**, broadening of the peaks at $\delta = 15.61$ ppm and 13.40 ppm attributable to the N-H and O-H protons, respectively was observed (**Fig. S15b**). Furthermore the peaks at δ 8.504, 7.8564, 7.3454 corresponding to H_b, H_c and H_i shifted to 8.5255, 7.8702 and 7.2957 respectively (**Fig. S14**).

Selectivity

The fluorescent response of organic moiety towards the different metal ions were investigated with 100 times concentration of alkali (Na(I), K(I)), alkaline earth (Mg(II), Ca(II)), and transition-metal ions (Ni(II), Zn(II), Cd(II), Co(II), Cu(II), Fe(II/III), Cr(III), Hg(II)) and Pb(II), Ag(I) (**Figs. S11** and **12**). It reveals that organic moiety has an excellent selectivity and specificity to Al(III) ion over other cations.

Effect of pH

The fluorescence intensity of organic moiety was measured at various pH values adjusting the pH using HEPES buffer in presence and absence of Al(III) ion. In the absence of Al(III) ion, organic moiety exhibited fluorescence of weak intensity and showed pH independency over the pH range 6.0 to 10.0 (**Fig. S16**). It is also noteworthy that the fluorescence intensity of the organic moiety in presence of Al(III) ion is higher than that in absence of Al(III) ion.

105 Analytical figure of merit

The detection limit was calculated from the calibration curve based on the fluorescence enhancement at 450 nm (**Fig. 6**) focusing on the lower concentration region of Al(III) ions. From the slope of the curve (S) and the standard deviation of

seven replicate measurements of the zero level (σ_{zero}), the detection limit was estimated using the equation $3\sigma/S$. The data from this graph indicates that this probe effectively detect Al(III) ion at very low level concentration (LOD = 31.78 nM)^{28,33}.

Cell Imaging

To examine the utility of the probe in biological systems, it was applied to human cervical cancer HeLa cell. Here, Al(III) and HL were allowed to uptake by the cells of interest and the images of the cells were recorded by fluorescence microscopy following excitation at ~ 405 nm (Fig. 7). In addition, the *in vitro* study showed that the probe, HL has not shown significant cytotoxic effect to the cells upto 8.0 h (IC₅₀ > 50 μM) (Fig. S17). These results indicate that the probe has a huge potentiality for both *in vitro* and *in vivo* application as Al(III) sensor as well as imaging in different ways as same manner for live cell imaging can be followed instead of fixed cells.

Conclusion

In conclusion, a new naphthelene-pyrazol conjugate (HL) has been designed and crystallographically characterized and it behaved as an Al(III) ions selective chemosensor sensor through ICT-CHEF processes in 100 mM HEPES buffer (water /DMSO:5/1, v/v) at biological pH. The processes have been supported by the electronic, fluorimetric and ¹HNMR titration. This probe is also useful to detect the Al(III) ions in HeLa cells as HL has no cytotoxicity. It is also noteworthy that this Al(III) ions selective probe associated with blue shift is superior to the previously reported blue shifting fluorescence probes^{30,34} in terms of the detection limit as here the LOD (31.78 nM) is lower than the earlier report(80 nM).³⁴

Acknowledgements

Financial support from Council of Scientific and Industrial Research (CSIR), New Delhi, India is gratefully acknowledged. M. Mukherjee and B. Sen wish to thank to UGC, New Delhi, India for offering the fellowships. We sincerely acknowledge Prof. Samita Basu and Mr. Ajay Das, Chemical Science Division, SINP, Kolkata, for enabling TCSPC instrument, Prof. B. Mukhopadhyay, IISER, Kolkata for providing the facility to record some ¹H NMR spectra and HR Mass Spectra and Prof. M. S. Hundal, Guru Nanak Dev University, Amritsar for crystallographic analysis. We are grateful to the honourable reviewers for their valuable comments for the improvement of this article.

45 Notes and references

^aDepartment of Chemistry, Burdwan University, Golapbag, Burdwan-713104, West Bengal, India, E-mail: pabitracc@yahoo.com

^bDepartment of Inorganic and Physical Chemistry, Indian Institute of Science, Bangalore, 560012, India

^cGovt. college of Engineering and Leather Technology, Salt Lake Sector-III, Kolkata 9

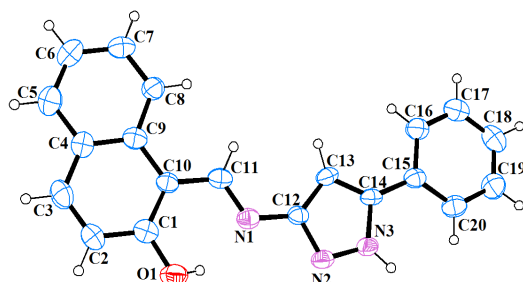
†Electronic Supplementary Information (ESI) available: See DOI: 10.1039/b000000x/

[‡]CCDC 994856 contains the supplementary crystallographic data for this paper. These data can be obtained free of charge from The

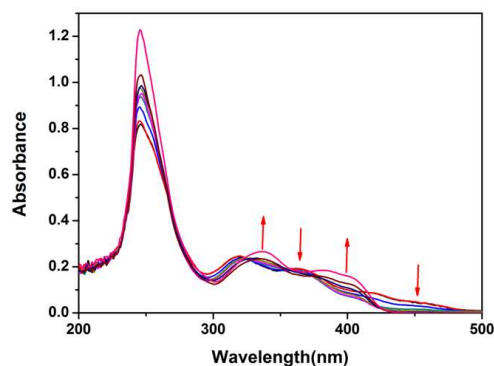
Cambridge Crystallographic Data Centre via http://www.ccdc.cam.ac.uk/data_request/cif.

- 60 1. W.S. Miller, L. Zhuang, J. Bottema, A.J. Wittebrood, P. De Smet, A. Haszler and A. Vieregge, *Mater. Sci. Eng. A.*, 2000, **280**, 37.
2. R.E. Doherty, *Environ. Forensics*, 2000, **1**, 83.
3. G. Ciardelli and N. Ranieri, *Water Res.*, 2001, **35**, 567.
4. R. Flarend, T. Bin, D. Elmore and S.L. Hemb, *Food Chem. Toxicol.* 2001, **39**, 163.
5. R.A. Yokel, *Food Chem. Toxicol.*, 2008, **46**, 2261.
6. J.L. Greger, *Crit. Rev. Clin. Lab. Sci.*, 1997, **34**, 439.
7. P.D. Darbre, A. Bakir and E. Iskakova, *J. Inorg. Biochem.*, 2013, **128**, 245.
8. (a) V. Rondeau, D. Commenges, H. Jacqmin-Gadda and J.F. Dartigues, *Am. J. Epidemiol.*, 2000, **152**, 59; (b) P.D. Darbre, F. Mannello and C. Exley, *J. Inorg. Biochem.*, 2013, **128**, 257 and refs. therein.
9. (a) M. Hemadi, G. Miquel, P.H. Kahn and J.M.E.H. Chahine, *Biochemistry*, 2003, **42**, 3120; (b) R.B. Martin, J. Savory, S. Brown, R.L. Bertholf and M.R. Wills, *Clin. Chem.*, 1987, **33**, 405; (c) A.J. Roskams and J.R. Connor, *Proc. Natl. Acad. Sci. USA*, 1990, **87**, 9024; (d) M. Cochran, V. Chawtur, M.E. Jones and E.A. Marshall, *Blood*, 1991, **77**, 2347; (e) S. Kim, J.Y. Noh, K.Y. Kim, J.H. Kim, H. K. Kang, S.W. Nam, S.H. Kim, S. Park, C. Kim and J. Kim, *Inorg. Chem.*, 2012, **51**, 3597 and refs. therein.
10. (a) G.D. Fasman, *Coord. Chem. Rev.*, 1996, **149**, 125; (b) P. Nayak, *Environ. Res.*, 2002, **89**, 101; (c) C.S. Cronan, W.J. Walker and P. R. Bloom, *Nature*, 1986, **324**, 140.
11. (a) G. Berthon, *Coord. Chem. Rev.*, 2002, **228**, 319; (b) A.M. Pierides, W.G. Edwards Jr, U.X. Cullum Jr, J.T McCall and H.A. Ellis, *Kidney Int.*, 1980, **18**, 115.
12. E.H. Jeffery, K. Abreo, E. Burgess, J. Cannata and J.L. Greger, *J. Toxicol. Env. Health*, 1996, **48**, 649.
13. A. Becaria, A. Campbell and S.C. Bondy, *Toxicol. Ind. Health*, 2002, **18**, 309.
14. J.J. Spinelli, P.A. Demers, N.D. Le, M.D. Friesen, M.F. Lorenzi, R. Fang and R.P. Gallagher, *Cancer Cause Control*, 2006, **17**, 939.
15. B. Armstrong, C. Tremblay, D. Baris and G. Theriault, *Am. J. Epidemiol.*, 1994, **139**, 250.
16. E. Álvarez, M.L. F-Marcos, C. Monterroso and M.J. F-Sanjurjo, *Ecol Manag.*, 2005, **211**, 227.
17. J. Barceló and C. Poschenrieder, *Environ Exp Bot*, 2002, **48**, 75.
18. (a) H. Lian, Y. Kang, S. Bi, Y. Arkin, D. Shao, D. Li, Y. Chen, L. Dai, N. Gan and L. Tian, *Talanta*, 2004, **62**, 43; (b) H. Seol, S.C. Shin and Y.B. Shim, *Electroanal.*, 2004, **16**, 2051; (c) O.Y. Nadzhafova, S.V. Lagodzinskaya and V.V. Sukhan, *J. Anal. Chem.*, 2001, **56**, 178; (d) A.J. Downard, B.O'Sullivan and K.J. Powell, *Anal. Chim. Acta*, 1997, **345**, 5; (e) M.J. Ahmed and J. Hossan, *Talanta*, 1995, **42**, 1135.
19. J.R. Lakowicz, *Principles of Fluorescence Spectroscopy*, Springer 2006.
20. (a) A.P. de Silva, D.B. Fox, J.M. Huxley and T.S. Moody, *Coord. Chem. Rev.*, 2000, **205**, 41; (b) B. Valeur and I. Leray, *Coord. Chem. Rev.*, 2000, **205**, 3.
21. (a) K. Dhara, U.C. Saha, A. Dan, M. Manassero, S. Sarkar and P. Chattopadhyay, *Chem. Commun.*, 2010, **46**, 1754; (b) U.C. Saha, K. Dhara, 60 B. Chattopadhyay, S.K. Mandal, S. Mondal, S. Sen, M. Mukherjee, S.V. Smaalen and P. Chattopadhyay, *Org. Lett.*, 2011, **13**, 4510; (c) U.C. Saha, B. Chattopadhyay, K. Dhara, S. K. Mandal, S. Sarkar, A.R. Khuda-Bukhsh, M. Mukherjee, M. Helliwell and P. Chattopadhyay, *Inorg. Chem.*, 2011, **50**, 1213; (d) S. Sen, T. Mukherjee, S. Sarkar, S.K. Mukhopadhyay and P. Chattopadhyay, *Analyst*, 2011, **136**, 4839; (e) S. Sen, T. Mukherjee, B. Chattopadhyay, A. Moirangthem, A. Basu, J. Marek and P. Chattopadhyay, *Analyst*, 2012, **137**, 3975; (f) M. Mukherjee, B. Sen, S. Pal, M. S. Hundal, S.K. Mandal, A.R.

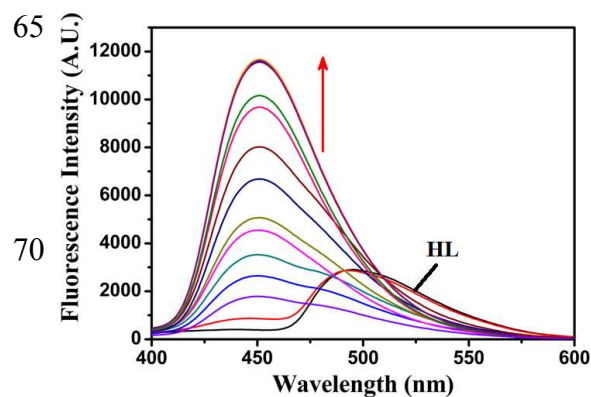
- 1 Khuda-Bukhsh and P. Chattopadhyay, *RSC Advances*, 2013, **3**,
 2 19978.
 3 22. B. Sen, S. Pal, S. Lohar, M. Mukherjee, S.K. Mandal, A.R. Khuda-
 4 Bukhsh and P. Chattopadhyay, *RSC Advances*, 2014, **4**, 21471 and
 5 references therein.
 6 23. A. Altomare, G. Cascarano, C. Giacovazzo and A. Guagliardi, *J.*
 7 *Appl. Crystallogr.*, 1993, **26**, 343.
 8 24. G.M. Sheldrick, *Acta Cryst. A*, 2008, **A64**, 112.
 9 25. L.J. Farrugia, *J. Appl. Cryst.*, 1999, **32**, 837.
 10 26. J.L. McClintock and B. P. Ceresa, *Invest. Ophthalmol. Vis. Sci.*,
 11 2010, **51**, 3455.
 12 27. (a) S. Banerjee, P. Prasad, A. Hussain, I. Khan, P. Kondaiah and A.
 13 R. Chakravarty, *Chem. Commun.*, 2012, **48**, 7702; (b) T.
 14 Mosmann, *J. Immunol. Methods*, 1983, **65**, 55.
 15 28 (a) S. Pal, B. Sen, M. Mukherjee, K. Dhara, E. Zangrando, S. K.
 16 Mandal, A.R. Khuda-Bukhsh and P. Chattopadhyay, *Analyst*,
 17 2014, **139**, 1628; (b) S. Madhu, M.R. Rao, M.S. Shaikh, M.
 18 Ravikanth, *Inorg. Chem.*, 2011, **50**, 4392.
 19 29. W.H. Melhuish, *J. Phys. Chem.*, 1961, **65**, 229
 20 30. D. Maity and T. Govindaraju, *Chem. Commun.*, 2010, **46**, 4499.
 21 31. H.A. Benesi and J.H. Hildebrand, *J. Am. Chem. Soc.*, 1949, **71**,
 22 2703.
 23 32. N.J. Turro, *Modern Molecular Photochemistry*; Benjamin/
 24 Cummings Publishing Co., Inc.: Menlo Park, CA, 1978, 246.
 25 33 M. Mukherjee, S. Pal, B. Sen, S. Lohar, S. Banerjee, S. Banerjee
 26 and P. Chattopadhyay, *RSC Adv.*, 2014, **4**, 27665.
 27 34 D. Karak, S. Lohar, A. Banerjee, A. Sahana, I. Hauli, S.K.
 28 Mukhopadhyay, J.S. Matalobos and D. Das, *RSC Adv.*, 2012, **2**,
 29 12447.



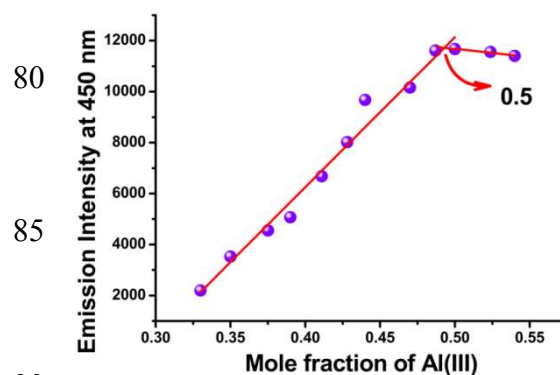
35 **Fig. 1** An ortep view of **HL** with atom numbering scheme (50%
 36 probability structure)



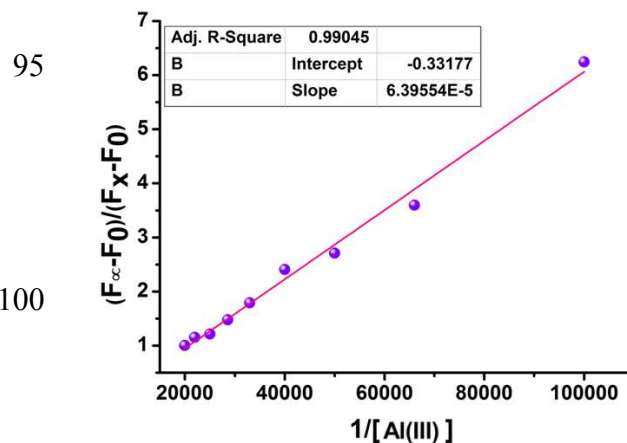
37 **Fig. 2** UV-Vis titration spectra of **HL** with Al(III) ions (0, 0.5, 1, 2, 3,
 38 4, 5, 6, 7, 8, 9, 10, 12, 15 μM respectively) in 100 mM HEPES
 39 buffer (DMSO/ water: 1/5) at 25 $^{\circ}\text{C}$



40 **Fig. 3** Fluorescence titration of **HL** with incremental addition of Al(III)
 41 ions (0, 0.5, 1, 2, 3, 4, 5, 6, 7, 8, 9, 10, 12, 15 μM respectively) in
 42 100 mM HEPES buffer (DMSO/ water: 1/5) at 25 $^{\circ}\text{C}$



43 **Fig. 4** Job's plot of **HL** from UV-Vis titration showing 1:1
 44 stoichiometry



45 **Fig. 5** Binding constant (K) value of $5.18 \times 10^3 \text{ M}^{-1}$ for **HL** determined
 46 from the intercept/slope of the Emission plot

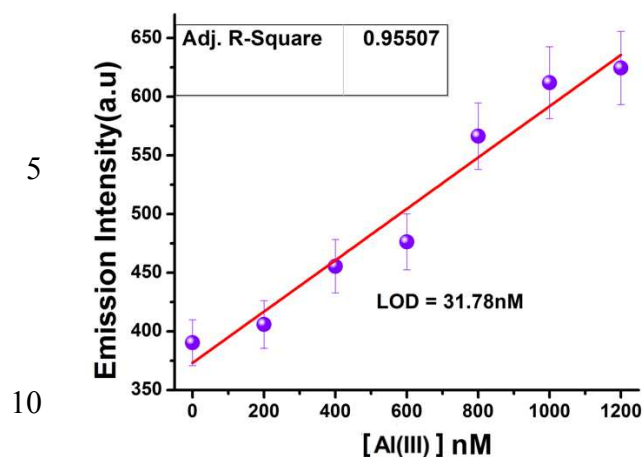
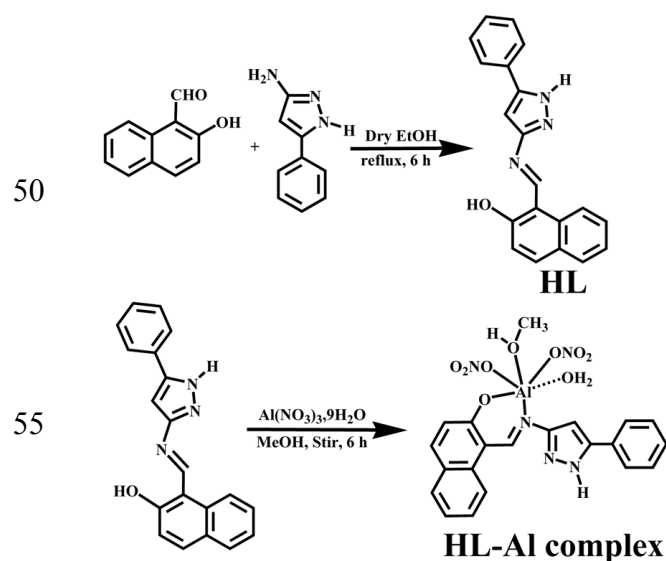


Fig. 6 Calibration curve for the nanomolar range, with error bars for calculating the LOD of Al(III) by HL in 100 mM HEPES buffer (DMSO/ water: 1/5) at 25 °C



Scheme 1 Schematic representation of synthesis of the probe HL and the corresponding HL-Al complex.

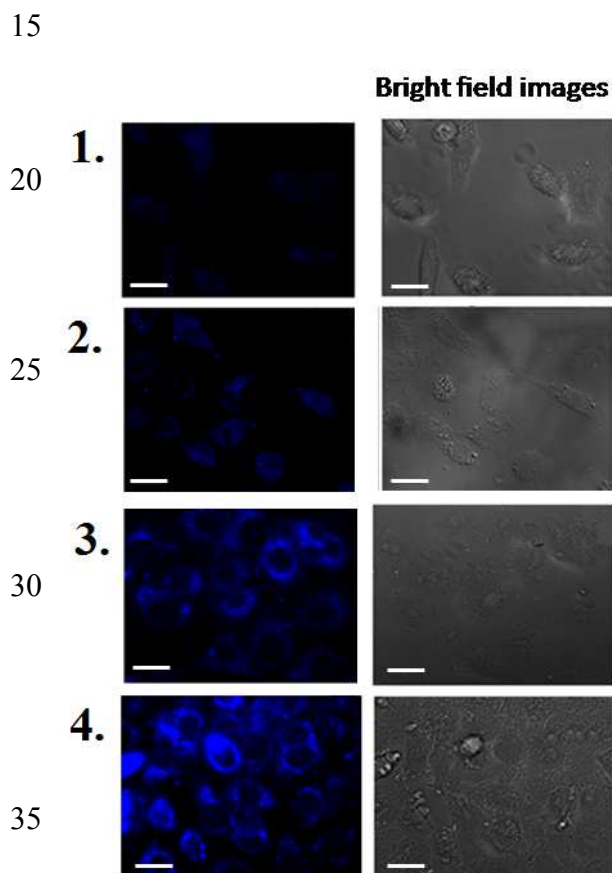
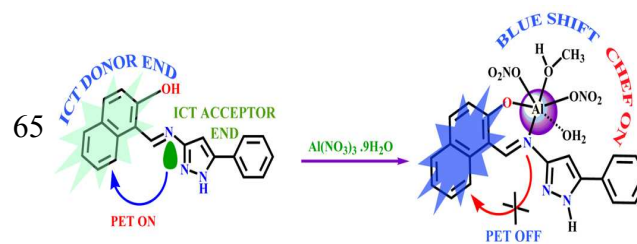


Fig. 7 Fluorescence image of HeLa cells (1) cells were incubated with 0 μM Al(III); (2) cells incubated with 2 μM Al(III) ; (3) cells incubated with 5 μM Al(III) solution; (4) cells incubated with 10 μM Al(III) All the samples were excited at 405 nm with emission 450 nm by using a [10 X] objective.



Scheme 2 Probable mechanistic pathway for sensing of Al(III) ions.

Table 1 Crystal data and details of refinements for **HL**

Bond length (Å)	
N(2)-N(3)	1.343(5)
N(3)-H(3A)	0.8600
O(1)-H(1)	0.8200
C(1)-O(1)	1.347(6)
C(11)-N(1)	1.294(5)
C(12)-N(1)	1.402(6)
C(14)-N(3)	1.365(5)
C(12)-N(2)	1.335(5)
Bond angles (°)	
O(1)-C(1)-C(10)	122.1(5)
O(1)-C(1)-C(2)	116.7(5)
N(1)-C(11)-C(10)	120.8(5)
N(1)-C(11)-H(11)	119.6
N(2)-C(12)-C(13)	112.2(5)
N(2)-C(12)-N(1)	114.4(4)
C(12)-N(2)-N(3)	103.6(4)
N(2)-N(3)-C(14)	113.0(4)
C(1)-O(1)-H(1)	109.5

Table 2 Selected bond distances (Å) and bond angles (°) for **HL**

Empirical Formula	C ₂₀ H ₁₅ N ₃ O
Formula Weight	313.36
Crystal system	orthorhombic
Space group	P 2 ₁ 2 ₁ 2 ₁
<i>a</i> (Å)	5.3994(12)
<i>b</i> (Å)	14.277(4)
<i>c</i> (Å)	20.499(5)
$\alpha = \beta = \gamma$	90°
Volume (Å ³)	1580.2(7)
Temperature (K)	296(2)
<i>Z</i>	4
ρ_{calc} (g/cm ³)	1.317
μ (mm ⁻¹)	0.084
F(000)	656
θ range (deg)	1.74 to 27.67°
Reflections collected	8503
Reflections independent	3602 [R(int) = 0.0979]
Final R indices [<i>I</i> > 2 σ (<i>I</i>)]	R1 = 0.0685, wR2 = 0.1189
Goodness-of-fit on <i>F</i> ²	0.917